



Article

Evaluation of the Properties, Gas Permeability, and Selectivity of Mixed Matrix Membrane Based on Polysulfone Polymer Matrix Incorporated with KIT-6 Silica

Sie Hao Ding ^{1,2}, Tiffany Yit Siew Ng ^{1,2}, Thiam Leng Chew ^{1,2,*} , Pei Ching Oh ^{1,2}, Abdul Latif Ahmad ³  and Chii-Dong Ho ⁴

¹ Department of Chemical Engineering, Universiti Teknologi PETRONAS, 32610 Seri Iskandar, Perak, Malaysia; ding.sie_g03642@utp.edu.my (S.H.D.); tiffany_16001691@utp.edu.my (T.Y.S.N.); peiching.oh@utp.edu.my (P.C.O.)

² CO₂ Research Centre (COSRES), Institute of Contaminant Management, Universiti Teknologi PETRONAS, 32610 Seri Iskandar, Perak, Malaysia

³ School of Chemical Engineering, Engineering Campus, Universiti Sains Malaysia, 14300 Nibong Tebal, Pulau Pinang, Malaysia; chlatif@usm.my

⁴ Department of Chemical and Materials Engineering, Tamkang University, New Taipei City 25137, Taiwan; cdho@mail.tku.edu.tw

* Correspondence: thiamleng.chew@utp.edu.my; Tel.: +605-3687626

Received: 19 September 2019; Accepted: 24 September 2019; Published: 23 October 2019



Abstract: Mixed matrix membranes (MMMs) separation is a promising technology for gas permeation and separation involving carbon dioxide (CO₂). However, finding a suitable type of filler for the formation of defect-free MMMs with enhancement in gas permeability remains a challenge. Current study focuses on synthesis of KIT-6 silica and followed by the incorporation of KIT-6 silica as filler into polysulfone (PSF) polymer matrix to fabricate MMMs, with filler loadings of 0–8 wt %. The effect of KIT-6 incorporation on the properties of the fabricated MMMs was evaluated via different characterization techniques. The MMMs were investigated for gas permeability and selectivity with pressure difference of 5 bar at 25 °C. KIT-6 with typical rock-like morphology was synthesized. Incorporation of 2 wt % of KIT-6 into PSF matrix produced MMMs with no void. When KIT-6 loadings in the MMMs were increased from 0 to 2 wt %, the CO₂ permeability increased by ~48%, whereas the ideal CO₂/CH₄ selectivity remained almost constant. However, when the KIT-6 loading in PSF polymer matrix was more than 2 wt %, the formation of voids in the MMMs increased the CO₂ permeability but sacrificed the ideal CO₂/CH₄ selectivity. In current study, KIT-6 was found to be potential filler for PSF matrix under controlled KIT-6 loading for gas permeation.

Keywords: KIT-6; polysulfone; MMMs; CO₂; gas permeability and selectivity

1. Introduction

Polymer membranes have been used industrially for gas separation. Their ease to scale-up, energy friendly, high efficiency, affordable, and simple operation make them economical favorable compared to conventional separation methods [1,2]. The common polymer membranes include cellulose acetate (CA), polyethersulfone (PESf), polyimide (PI), and polycarbonates (PC). Apart from these, polysulfone (PSF) is gaining great attention in recent years because PSF exhibits some important benefits such as good thermomechanical stability, high plasticization resistance (above 30 bar), and good gas permeability and selectivity [3–8].

In recent years, mixed matrix membranes (MMMs) emerged as alternative candidates for gas permeation and separation [9–13]. MMMs, comprising inorganic materials embedded in a polymer matrix, combine the ease of processability of polymers with high permeability or selectivity of inorganic porous fillers [14]. Furthermore, by incorporating inorganic fillers into polymer matrix, there is extremely huge possibility a membrane with higher gas separation performance relative to the bare polymeric membrane material can be established [15].

There is various type of inorganic materials have been used as fillers in polymer matrix, for instance, carbon nanotubes, zeolites, carbon molecular sieves, and metal–organic frameworks. Nevertheless, the production of defect-free MMMs is challenging because of the incompatibility in physical and chemical properties between the polymer and inorganic phase. Microvoid formation resulting from weak interaction between polymer and filler may cause membrane separation performance decreases significantly [14,15].

Ordered mesoporous silica materials, such as MCM-41 and MCM-48, are inorganic materials used as fillers in MMMs to enhance the gas separation performance of membranes. These mesoporous materials possess several advantages such as high CO₂ adsorption, high specific surface area, high mechanical and thermal stability. The high porosity of these materials facilitates the gas diffusion during gas separation [14].

In contrast to MCM-41 and MCM-48, KIT-6 is another type of larger pore size (~6 nm) mesoporous silica with a three-dimensional interconnected cubic pore structure. KIT-6 has been proved to have high affinity for various gases with its two intertwined systems of mesoporous channels which can also be connected via irregular micropores in the walls [16]. The large pore size of KIT-6 enables the formation of intimate composites, resulting from the penetration of polymer chain into the mesopores. Besides, the gas permeability can be enhanced due to easier diffusibility of gases through the large pore.

A numbers of studies have investigated the preparation and gas permeation studies of MMMs incorporated with mesoporous silica as filler. The incorporation of different type of fillers had different effects on the properties and the gas permeability of the formed MMMs. Wu et al. [17] investigated the CO₂ permeability of poly(ether-block-amide) incorporated with MCM-41. The CO₂ permeability was enhanced by 102.3% at 20 wt % filler loading of the MMMs [17]. Kim and Marrand [18] reported that incorporation of 40 wt % of MCM-41 into PSF increased the CO₂ permeability by 275% compared to pristine PSF. Jomekian et al. [19] prepared the MMMs of PSF incorporated with MCM-48 increased the CO₂ permeability by ~193% compared to pristine PSF. These studies show that incorporation of mesoporous silica into polymer membranes could enhance the gas permeability of the membranes.

In the current project, KIT-6 was used as filler with the aim to improve the CO₂ gas permeability of PSF polymer matrix. Different loadings of 0–8 wt % of KIT-6 silica were incorporated into PSF polymer matrix to fabricate MMMs. The synthesized KIT-6 was characterized using field-emission scanning microscopy (FESEM), X-ray diffraction (XRD), high-resolution transmission electron microscopy (HRTEM), and N₂ adsorption–desorption techniques. The effects of KIT-6 loading on the properties of fabricated MMMs were evaluated by characterization on the MMMs via FESEM and thermal gravimetric analysis (TGA). The fabricated MMMs were tested for gas permeability and selectivity at pressure difference of 5 bar.

2. Materials and Methods

2.1. Synthesis of KIT-6 Silica

KIT-6 silica was synthesized with the procedure reported previously with some modifications [20]. Pluronic P123 was dissolved in distilled water and concentrated hydrochloric acid (HCl, 37%) at 35 °C. After P123 was completely dissolved, butanol (BuOH) was added and stirred for an hour, followed by the addition of tetraethyl orthosilicate (TEOS). The resultant mixture is composed of TEOS:P123:HCl:H₂O:BuOH in a 1:0.017:4.948:188:1.31 mole ratio. After 24 h of stirring, the mixture was hydrothermally treated under static condition at 35 °C for 24 h. Next, the mixture was filtered and

washed with deionized water and followed by drying at 100 °C overnight in an oven. After drying, the sample was calcined for 6 h at 550 °C.

2.2. Fabrication of the Membranes

For pristine PSF membrane fabrication, 3.1235 g of PSF pellets (average MW ~35,000 by LS; average Mn ~16,000 by MO) were added to 10 mL of tetrahydrofuran (THF) and stirred for 18 h using a magnetic bar. After PSF pellets were completely dissolved, the dope solution was subjected to sonication to remove trapped bubbles for 30 min. Then, the dope solution was casted on a glass plate by using casting knife. The polymer on the glass plate was covered and left 3 days in room temperature to ensure complete solvent evaporation. Then, the membrane was peeled off and stored for future usage.

For MMM fabrication, various loadings (2, 4, 6, 8 wt %) of KIT-6 were added, respectively, to 10 mL of THF followed by 30 min of ultrasonication. Then, PSF pellets were added and dissolved into KIT-6 solution for 24 h using a magnetic bar. After mixing for 18 h, the dope solution was subjected to sonication to remove trapped bubbles for 30 min. Then, the dope solution was casted on a glass plate by using casting knife. The MMMs on the glass plate were covered and left 3 days in room temperature to ensure complete solvent evaporation. The MMMs were peeled off and stored for future usage. The fabricated MMMs were named as 2%-KIT-6/PSF, 4%-KIT-6/PSF, 6%-KIT-6/PSF, and 8%-KIT-6/PSF for MMMs incorporated with KIT-6 loadings of 2, 4, 6, and 8 wt %, respectively.

2.3. KIT-6 Characterization

KIT-6 was subjected to X-ray diffraction (XRD, X'Pert³ Powder & Empyrean, PANalytical) scanning from 0.8 ° to 6 ° (2 theta) for crystalline structure study. The pore structure of KIT-6 was observed using high-resolution transmission electron microscopy (HRTEM, FEI Tecnai 20). The surface morphology of KIT-6 was revealed by using field-emission scanning electron microscope (FESEM, Zeiss Supra55 VP). N₂ adsorption–desorption studies (TriStar II 3020) using liquid at nitrogen temperature of 77 K was used to study the pore characteristic of KIT-6. The specific surface area of KIT-6 was determined by using the Brunauer–Emmett–Teller (BET) technique. The mesopore pore size distribution was determined by using the Barrett–Joyner–Halenda (BJH) technique.

2.4. Membranes Characterization

The morphologies of the prepared membranes were analyzed by FESEM. Liquid nitrogen was used to break the pristine PSF membrane and KIT-6/PSF membranes to prepare a cross section of the membrane for FESEM analysis. Thermal gravimetric analysis (TGA, Perkin Elmer, STA-6000) with heating rate of 10 °C/min in nitrogen gas was used to study the weight change of the membranes with increasing temperature.

2.5. Gas Permeability and Selectivity Study

The gas permeability and selectivity study was carried out by feeding single gas CO₂ gas and CH₄ with 99.99% purity to the membrane. The membrane was sealed in a stainless steel permeation cell with permeate pressure of 1 bar. The feed pressure was regulated so that the pressure difference was 5 bar. The permeate flow was measured using bubble flow meter. The gas permeability was calculated using Equation (1).

$$P = \frac{Nl}{(P_f - P_p)A} \quad (1)$$

where P is gas permeability across the membrane (Barrer, 1×10^{-10} cm³ (STP) cm/[cm² s cmHg]), N is the permeate flow (cm³ s⁻¹), l is membrane thickness (cm), A is the membrane area (cm²), P_f is the feed pressure (cm Hg), and P_p is the permeate pressure (cmHg).

The ideal selectivity, α^i , of the membrane was calculated using Equation (2).

$$\alpha^i_{CO_2/CH_4} = P_{CO_2}/P_{CH_4} \quad (2)$$

3. Results and Discussion

3.1. Characterization of KIT-6

The powder XRD pattern of KIT-6 is shown in Figure 1. The peak at 1.09° shows that the sample possesses ordered mesostructure with a three-dimensional cubic Ia3d symmetry [16,21]. The XRD patterns represent two reflections, which can be assigned to (211) and (332). The XRD pattern of the KIT-6 sample synthesized in the current project agreed with the XRD pattern of KIT-6 reported by Ayad et al. [21].

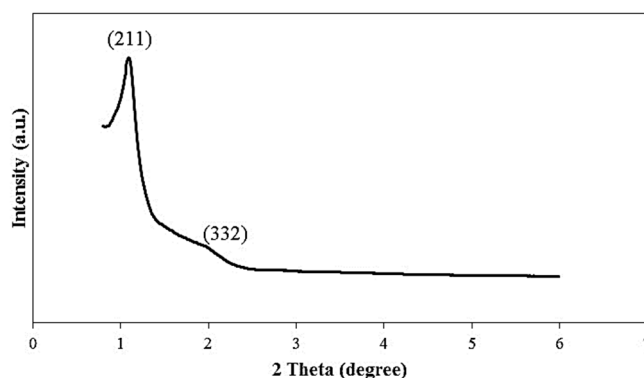


Figure 1. XRD pattern of KIT-6.

Figure 2 shows the HRTEM images of synthesized KIT-6. The gyroidal cubic Ia3d structure of KIT-6 is observed in the HRTEM image in Figure 2 [22]. Figure 3 shows the FESEM image of the KIT-6. The FESEM image shows that the morphology of KIT-6 is typical rock-like morphology [14,15,23].

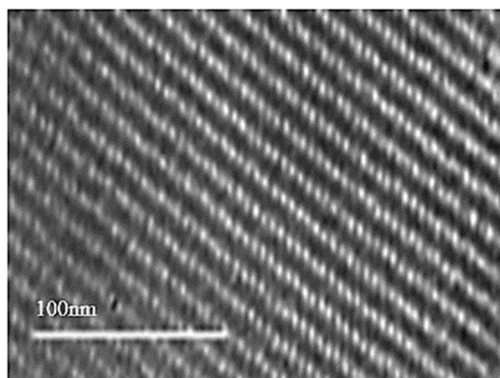


Figure 2. HRTEM image of KIT-6.

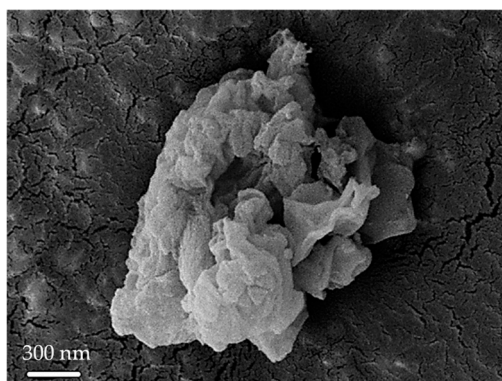


Figure 3. Field-emission scanning electron microscopy (FESEM) image of KIT-6.

The nitrogen adsorption–desorption isotherm of KIT-6 is shown in Figure 4. From the nitrogen adsorption isotherms of KIT-6, type IV with a hysteresis loop can be observed which proved the characteristic of a mesoporous material [15,16,19,22,24]. The specific surface area, pore volume, and pore diameter of KIT-6 were determined to be 585 m²/g, 0.42 cm³/g, and 7.01 nm, respectively, which agreed with the data reported by Kishor & Ghoshal [22].

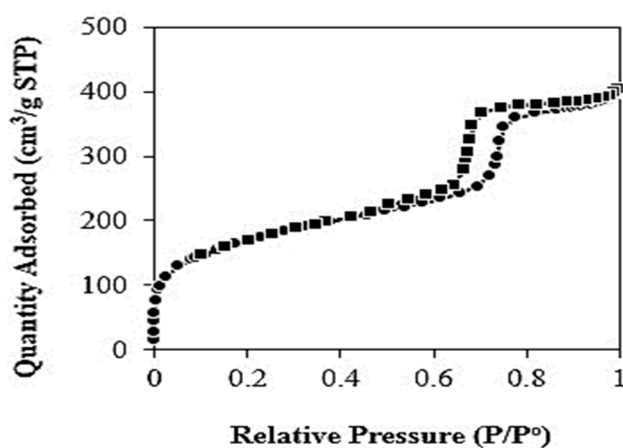


Figure 4. Nitrogen adsorption–desorption isotherm of KIT-6.

3.2. Membrane Characterization

Table 1 shows the weight loss percentage of the membranes via TGA analysis. Generally, weight loss occurred in 3 stages. In the first stage, desorption of physically absorbed water occurred at 30–500 °C. The main thermal degradation occurred from 500 to 580 °C. Most of the weight loss in the membranes occurred in this stage. Finally, at 580–800 °C, the samples were decomposed into ash. For pristine PSF membrane, the substantial weight loss started at around 500 °C which agreed with the onset temperature reported by other researchers [15,25,26]. MMMs with KIT-6 fillers also showed similar decomposition temperature with no obvious changes.

Table 1. Weight loss percentage of membranes via TGA analysis [15,25,26].

Membrane Samples	Weight Percentage Loss (%)			Total Weight Loss
	Desorption of Absorbed Water at 30–500 °C	Main Thermal Degradation at 500–580 °C	Decomposition into Ash at 580–800 °C	
Pristine PSF	2.5	54.5	15.8	72.8
2%-KIT-6/PSF	4.4	64.2	13.5	82.1
4%-KIT-6/PSF	4.0	55.2	12.2	71.4
6%-KIT-6/PSF	1.7	54.3	10.0	66.0
8%-KIT-6/PSF	1.9	48.9	11.8	62.6

Figure 5 shows FESEM images of surface morphology for pristine PSF membrane and MMMs. Smooth and clear surface morphology is observed for pristine PSF membrane in Figure 5a. It is observed that serious agglomeration of KIT-6 is observed in the MMMs when the KIT-6 loading was at 8 wt %.

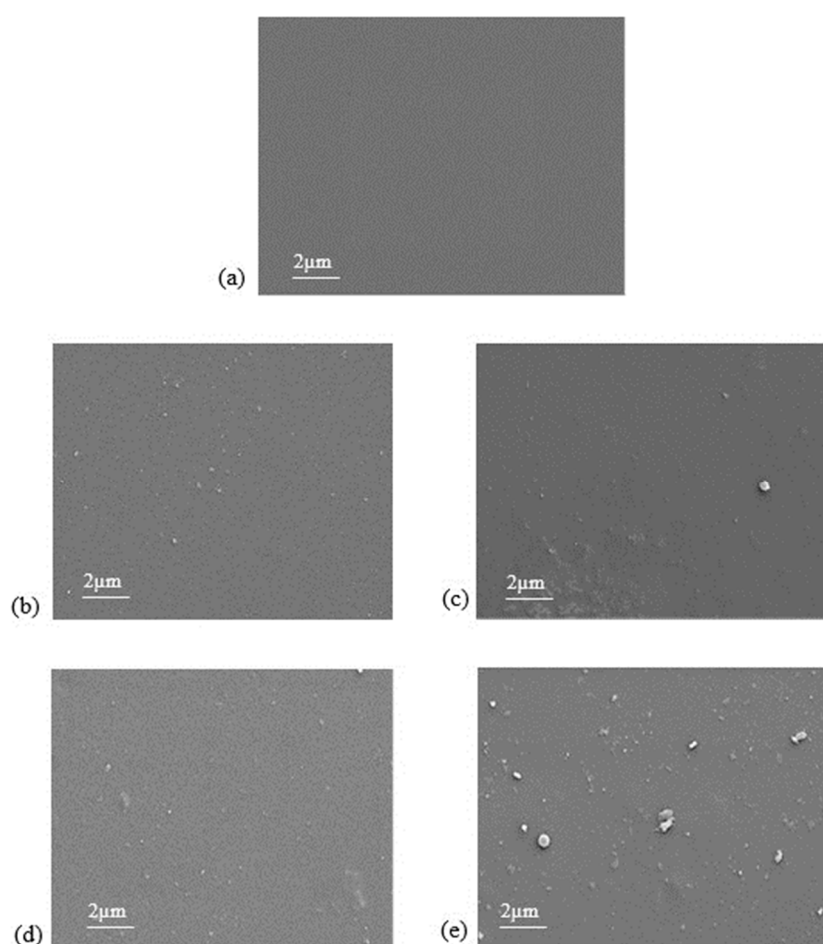


Figure 5. The top view FESEM images of (a) pristine polysulfone (PSF) membrane; (b) 2%-KIT-6/PSF; (c) 4%-KIT-6/PSF; (d) 6%-KIT-6/PSF; and (e) 8%-KIT-6/PSF.

Figure 6 shows FESEM images of the cross-sectional morphology of pristine PSF membrane and MMMs. A dense structure can be seen in the pristine PSF membrane as shown in Figure 6a. No void was found for MMMs when 2 wt % of KIT-6 were incorporated into PSF matrix. However, serious void formation was observed in the MMMs when the KIT-6 loading was more than 4 wt %. This might be due to the occurrence of KIT-6 agglomeration at higher loading, which disturbed the PSF polymer

matrix. The hydroxyl group attached on surface of silica caused KIT-6 tend to agglomerate with each other easily via hydrogen bonding [14,18,19].

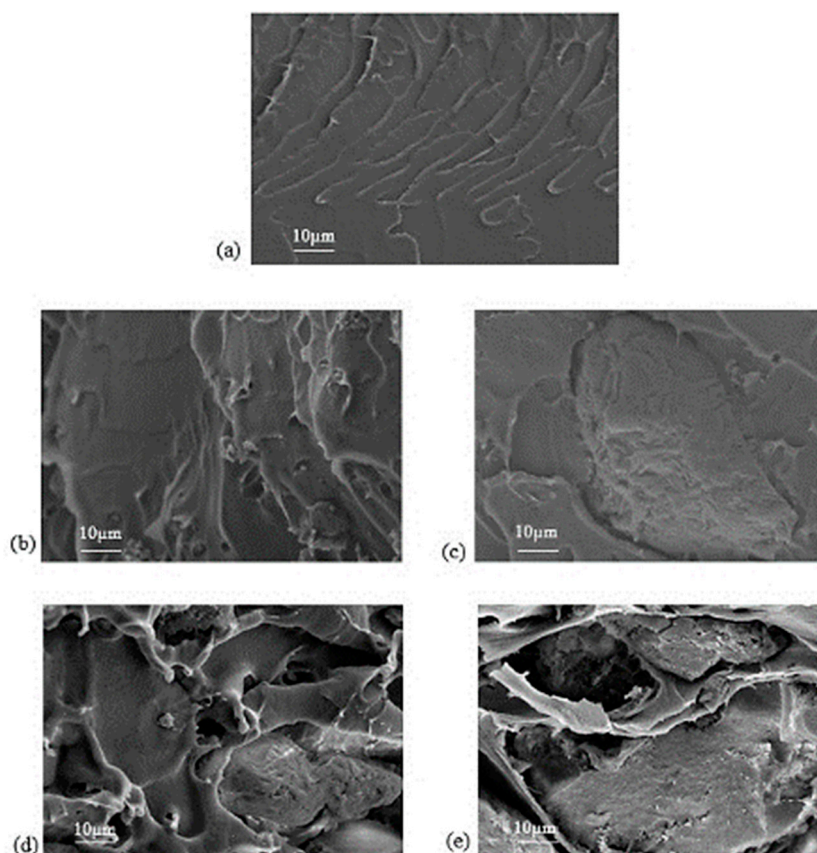


Figure 6. The cross-sectional images of (a) pristine PSF membrane; (b) 2%-KIT-6/PSF; (c) 4%-KIT-6/PSF; (d) 6%-KIT-6/PSF; and (e) 8%-KIT-6/PSF.

3.3. CO₂ Permeability and Selectivity of the Membranes

Figure 7 shows the CO₂ permeability of the membranes, whereas Figure 8 shows the ideal CO₂/CH₄ selectivity at different KIT-6 loadings. When KIT-6 loadings in the MMMs were increased from 0 to 2 wt %, the CO₂ permeability increased by ~48%, whereas the ideal CO₂/CH₄ selectivity is observed to be almost constant. The increase of CO₂ diffusivity was due to preferable permeation of CO₂ through the three-dimensional mesopores of KIT-6 loaded into the MMMs and the disruption of polymer chain packing in the presence of KIT-6 filler [16]. When the KIT-6 loading was increased to 2 wt %, more CO₂ was able to permeate through the mesopores of KIT-6 in the MMMs [14,27]. On the other way, the CO₂ permeability increased, but the ideal CO₂/CH₄ selectivity decreased when KIT-6 loading was more than 2 wt %, which could be due to the voids formation in the MMMs. The void formation became more serious when the KIT-6 loading was increased to beyond 4 wt %, as observed from FESEM images of cross-sectional morphology in Figure 6d,e [28]. The formed voids between the KIT-6 and PSF matrix might create bypassing channels for the permeation of the gas molecules. Consequently, the gas molecules tend to pass through the bypassing channels created by the voids in the MMMs with less resistance instead of passing through the mesoporous pore channel of KIT-6. This leaky interface caused increase in the gases permeability of membrane but sacrificing the ideal CO₂/CH₄ selectivity when the KIT-6 loading was more than 2 wt % [29].

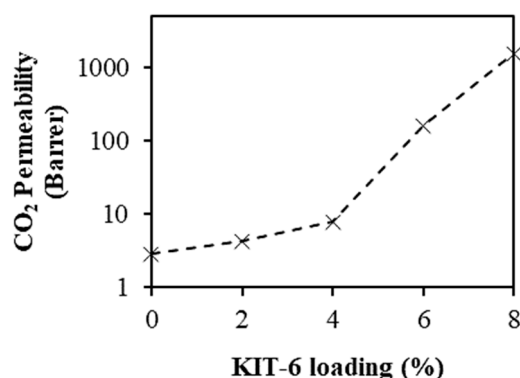


Figure 7. Effect of KIT-6 loading on CO₂ permeability at 5 bar pressure difference and 25 °C.

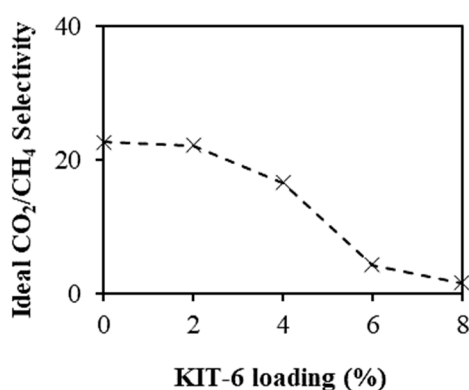


Figure 8. Effect of KIT-6 loading on CO₂/CH selectivity at 5 bar pressure difference and 25 °C.

Several researches have reported on the usage of MMMs incorporated by mesoporous silica for CO₂ gas permeation. Waheed et al. [27] reported that the CO₂ permeability increased ~6% when the PSF membrane was incorporated with 10 wt % rice husk silica (RHS) filler. Besides, the increment in CO₂ permeability of ~89% was also reported by Kim and Marrand [30] when 10 wt % of MCM-48 was incorporated into the PSF polymer. Khan et al. [28] also reported that CO₂ permeability was increased ~16% when Matrimid polymer was incorporated with 10 wt % of MCM-41 silica. On the other hand, Khan et al. [31] presented that the CO₂ permeability raised for about 21% by incorporating 10 wt % of COK-12 into Matrimid polymer.

Research works have also reported on CO₂ gas permeation using MMMs incorporated by fillers, which are other than mesoporous silica. Pakizeh et al. [32] reported increment of CO₂ permeability of ~8% when 20 wt % 4A was incorporated into PSF polymer. On the other hand, Feijani et al. [33] incorporated MIL-53 into poly(vinylidene fluoride) based MMMs and CO₂ permeability increased by ~32% when 5% of MIL-53 was incorporated into the MMMs. In another research work reported by Perez et al. [34], an approximately 28% increase in CO₂ permeability was achieved when 23 wt % of MOP-18 was incorporated into Matrimid-based MMMs. In the current study, the ~48% increase in CO₂ permeability, obtained by incorporating 2 wt % of KIT-6 into the MMMs, appears to be higher compared with the increase in CO₂ permeability reported in many of the above-mentioned studies.

4. Conclusions

KIT-6 with typical rock-like morphology was synthesized and incorporated into the PSF matrix to form MMMs. The occurrence of serious agglomeration of KIT-6 in the MMMs is observed at KIT-6 loading of 8 wt %. Incorporation of 2 wt % of KIT-6 into PSF matrix produced MMMs with no void. When KIT-6 loadings in the MMMs were increased from 0 to 2 wt %, the CO₂ permeability increased by ~48%, whereas the ideal CO₂/CH₄ selectivity remained almost constant. When KIT-6 loading was increased up to 2 wt %, the increase in CO₂ permeability was due to preferable permeation of CO₂ through the three-dimensional mesopores of KIT-6 loaded into the MMMs and the disruption of polymer chain packing in the presence of KIT-6 filler. Therefore, current study indicates that KIT-6 is potential filler for MMMs fabrication under controlled KIT-6 loading in order to increase the CO₂ gas permeability performance of the membranes.

Author Contributions: Conceptualization, T.L.C. and P.C.O.; Methodology, S.H.D. and T.L.C.; Investigation, S.H.D.; Analysis, S.H.D., T.L.C., and P.C.O.; Supervision, T.L.C., P.C.O., and A.L.A.; writing—original draft, S.H.D.; writing – review and editing, T.Y.S.N., T.L.C., P.C.O., A.L.A., and C.-D.H.

Funding: This research was funded by Long Term Research Grant Scheme (LRGS), grant number 304/PJKIMIA/6050296/U124 and YUTP-Fundamental Research Grant (Cost center: 0153AA-H43).

Acknowledgments: This research work was supported by Universiti Teknologi PETRONAS, Institute Contaminant Management UTP and CO₂ Research Centre (CO₂RES). The authors would also like to acknowledge the technical and financial support from Long Term Research Grant Scheme (LRGS) (cost center: 0153AB-L12). The author would also like to acknowledge the financial support from YUTP-Fundamental Research Grant (Cost center: 0153AA-H43).

Conflicts of Interest: The authors declare no conflicts of interest. The funders had no role in the design of the study; in the collection, analyses, or interpretation of data; in the writing of the manuscript; or in the decision to publish the results.

References

1. Kinoshita, Y.; Wakimoto, K.; Gibbons, A.H.; Isfahani, A.P.; Kusuda, H.; Sivaniah, E.; Ghalei, B. Enhanced PIM-1 membrane gas separation selectivity through efficient dispersion of functionalized POSS fillers. *J. Membr. Sci.* **2017**, *539*, 178–186. [[CrossRef](#)]
2. Yavari, M.; Okamoto, Y.; Lin, H. The role of halogens in polychlorotrifluoroethylene (PCTFE) in membrane gas separations. *J. Membr. Sci.* **2018**, *548*, 380–389. [[CrossRef](#)]
3. Mohamad, M.B.; Fong, Y.Y.; Shariff, A. Gas separation of carbon dioxide from methane using polysulfone membrane incorporated with Zeolite-T. *Procedia Eng.* **2016**, *148*, 621–629. [[CrossRef](#)]
4. Aroon, M.; Ismail, A.; Montazer-Rahmati, M.; Matsuura, T. Morphology and permeation properties of polysulfone membranes for gas separation: Effects of non-solvent additives and co-solvent. *Sep. Purif. Technol.* **2010**, *72*, 194–202. [[CrossRef](#)]
5. Bastani, D.; Esmaeili, N.; Asadollahi, M. Polymeric mixed matrix membranes containing zeolites as a filler for gas separation applications: A review. *J. Ind. Eng. Chem.* **2013**, *19*, 375–393. [[CrossRef](#)]
6. Brunetti, A.; Scura, F.; Barbieri, G.; Drioli, E. Membrane technologies for CO₂ separation. *J. Membr. Sci.* **2010**, *359*, 115–125. [[CrossRef](#)]
7. Wang, X.; Chen, H.; Zhang, L.; Yu, R.; Qu, R.; Yang, L. Effects of coexistent gaseous components and fine particles in the flue gas on CO₂ separation by flat-sheet polysulfone membranes. *J. Membr. Sci.* **2014**, *470*, 237–245. [[CrossRef](#)]
8. Shahid, S.; Nijmeijer, K. Matrimid®/polysulfone blend mixed matrix membranes containing ZIF-8 nanoparticles for high pressure stability in natural gas separation. *Sep. Purif. Technol.* **2017**, *189*, 90–100. [[CrossRef](#)]
9. Venturi, D.; Grupkovic, D.; Sisti, L.; Baschetti, M.G. Effect of humidity and nanocellulose content on Polyvinylamine-nanocellulose hybrid membranes for CO₂ capture. *J. Membr. Sci.* **2018**, *548*, 263–274. [[CrossRef](#)]
10. Bera, B.; Das, J.K.; Das, N. Mesoporous silica based composite membrane formation by in-situ cross-linking of phenol and formaldehyde at room temperature for enhanced CO₂ separation. *Microporous Mesoporous Mater.* **2018**, *256*, 177–189. [[CrossRef](#)]

11. Shete, M.; Kumar, P.; Bachman, J.E.; Ma, X.; Smith, Z.P.; Xu, W.; Mkhoyan, A.; Long, J.R.; Tsapatsis, M. On the direct synthesis of Cu (BDC) MOF nanosheets and their performance in mixed matrix membranes. *J. Membr. Sci.* **2018**, *549*, 312–320. [[CrossRef](#)]
12. Benavides, M.E.; David, O.; Johnson, T.; Łozińska, M.M.; Orsi, A.; Wright, P.A.; Mastel, S.; Hillenbrand, R.; Kapteijn, F.; Gascon, J. High performance mixed matrix membranes (MMMs) composed of ZIF-94 filler and 6FDA-DAM polymer. *J. Membr. Sci.* **2018**, *550*, 198–207. [[CrossRef](#)]
13. Sakaguchi, T.; Nakao, S.; Irie, S.; Hashimoto, T. Gas permeability of mixed matrix membranes composed of poly(diphenylacetylene)s and dispersed metal chloride particles. *Polymer* **2018**, *140*, 208–214. [[CrossRef](#)]
14. Khan, A.L.; Klaysom, C.; Gahlaut, A.; Vankelecom, I.F. Polysulfone acrylate membranes containing functionalized mesoporous MCM-41 for CO₂ separation. *J. Membr. Sci.* **2013**, *436*, 145–153. [[CrossRef](#)]
15. Tzi, E.C.N.; Ching, O.P. Surface modification of AMH-3 for development of mixed matrix membranes. *Procedia Eng.* **2016**, *148*, 86–92. [[CrossRef](#)]
16. Wang, J.; Li, Y.; Zhang, Z.; Hao, Z. Mesoporous KIT-6 silica–polydimethylsiloxane (PDMS) mixed matrix membranes for gas separation. *J. Mater. Chem. A* **2015**, *3*, 8650–8658. [[CrossRef](#)]
17. Wu, H.; Li, X.Q.; Li, Y.F.; Wang, S.F.; Guo, R.L.; Jiang, Z.Y.; Wu, C.; Xin, Q.P.; Lu, X. Facilitated transport mixed matrix membranes incorporated with amine functionalized MCM-41 for enhanced gas separation properties. *J. Membr. Sci.* **2014**, *465*, 78–90. [[CrossRef](#)]
18. Kim, S.; Marand, E. High permeability nano-composite membranes based on mesoporous MCM-41 nanoparticles in a polysulfone matrix. *Microporous Mesoporous Mater.* **2008**, *114*, 129–136. [[CrossRef](#)]
19. Jomekian, A.; Pakizeh, M.; Mansoori, S.; Poorafshari, M.; Hemmati, M.; Ataee Dil, P. Gas transport behavior of novel modified MCM-48/polysulfone mixed matrix membrane coated by PDMS. *J. Membr. Sci. Technol.* **2011**, *1*, 1–6.
20. Qian, L.; Ren, Y.; Liu, T.; Pan, D.; Wang, H.; Chen, G. Influence of KIT-6's pore structure on its surface properties evaluated by inverse gas chromatography. *Chem. Eng. J.* **2012**, *213*, 186–194. [[CrossRef](#)]
21. Ayad, M.M.; Salahuddin, N.A.; El-Nasr, A.A.; Torad, N.L. Amine-functionalized mesoporous silica KIT-6 as a controlled release drug delivery carrier. *Microporous Mesoporous Mater.* **2016**, *229*, 166–177. [[CrossRef](#)]
22. Kishor, R.; Ghoshal, A.K. APTES grafted ordered mesoporous silica KIT-6 for CO₂ adsorption. *Chem. Eng. J.* **2015**, *262*, 882–890. [[CrossRef](#)]
23. Hafizi, H.; Chermahini, A.N.; Saraji, M.; Mohammadnezhad, G. The catalytic conversion of fructose into 5-hydroxymethylfurfural over acid-functionalized KIT-6, an ordered mesoporous silica. *Chem. Eng. J.* **2016**, *294*, 380–388. [[CrossRef](#)]
24. Loganathan, S.; Ghoshal, A.K. Amine tethered pore-expanded MCM-41: A promising adsorbent for CO₂ capture. *Chem. Eng. J.* **2017**, *308*, 827–839. [[CrossRef](#)]
25. Ahn, J.; Chung, W.-J.; Pinnau, I.; Guiver, M.D. Polysulfone/silica nanoparticle mixed-matrix membranes for gas separation. *J. Membr. Sci.* **2008**, *314*, 123–133. [[CrossRef](#)]
26. Zornoza, B.; Irusta, S.; Téllez, C.; Coronas, J. Mesoporous silica sphere–polysulfone mixed matrix membranes for gas separation. *Langmuir* **2009**, *25*, 5903–5909. [[CrossRef](#)]
27. Waheed, N.; Mushtaq, A.; Tabassum, S.; Gilani, M.A.; Ilyas, A.; Ashraf, F.; Jamal, Y.; Bilad, M.R.; Khan, A.U.; Khan, L.A. Mixed matrix membranes based on polysulfone and rice husk extracted silica for CO₂ separation. *Sep. Purif. Technol.* **2016**, *170*, 122–129. [[CrossRef](#)]
28. Khan, A.L.; Klaysom, C.; Gahlaut, A.; Khan, A.U.; Vankelecom, I.F. Mixed matrix membranes comprising of Matrimid and–SO₃H functionalized mesoporous MCM-41 for gas separation. *J. Membr. Sci.* **2013**, *447*, 73–79. [[CrossRef](#)]
29. Rezakazemi, M.; Amooghin, A.E.; Montazer-Rahmati, M.M.; Ismail, A.F.; Matsuura, T. State-of-the-art membrane based CO₂ separation using mixed matrix membranes (MMMs): An overview on current status and future directions. *Prog. Polym. Sci.* **2014**, *39*, 817–861. [[CrossRef](#)]
30. Kim, S.; Marand, E.; Ida, J.; Gulians, V.V. Polysulfone and mesoporous molecular sieve MCM-48 mixed matrix membranes for gas separation. *Chem. Mater.* **2006**, *18*, 1149–1155. [[CrossRef](#)]
31. Khan, A.L.; Sree, S.P.; Martens, J.A.; Raza, M.T.; Vankelecom, I.F. Mixed matrix membranes comprising of matrimid and mesoporous COK-12: Preparation and gas separation properties. *J. Membr. Sci.* **2015**, *495*, 471–478. [[CrossRef](#)]

32. Pakizeh, M.; Hokmabadi, S. Experimental study of the effect of zeolite 4A treated with magnesium hydroxide on the characteristics and gas-permeation properties of polysulfone-based mixed-matrix membranes. *J. Appl. Polymer Sci.* **2017**, *134*, 1–7. [[CrossRef](#)]
33. Feijani, E.A.; Mahdavi, H.; Tavasoli, A. Poly(vinylidene fluoride) based mixed matrix membranes comprising metal organic frameworks for gas separation applications. *Chem. Eng. Res. Des.* **2015**, *96*, 87–102. [[CrossRef](#)]
34. Perez, E.V.; Balkus, K.J., Jr.; Ferraris, J.P.; Musselman, I.H. Metal-organic polyhedra 18 mixed-matrix membranes for gas separation. *J. Membr. Sci.* **2014**, *463*, 82–93. [[CrossRef](#)]



© 2019 by the authors. Licensee MDPI, Basel, Switzerland. This article is an open access article distributed under the terms and conditions of the Creative Commons Attribution (CC BY) license (<http://creativecommons.org/licenses/by/4.0/>).